

Nature of baryon resonances from LQCD, complementing experiment and EFT

Valery Lyubovitsky

Institut für Theoretische Physik, Eberhard Karls Universität Tübingen



in collaboration with

Stan Brodsky, SLAC
Thomas Gutsche, TU
Rich Lebed, ASU
Igor Obukhovsky, MSU
Ivan Schmidt, UTFSM
Alfredo Vega, UTFSM

INT Workshop “Spectrum and Structure of Excited Nucleons” UW, Seattle, 14-18 Nov 2016

Plan of the Talk

- Introduction: a few examples how Lattice QCD complements EFTs
- Three examples of EFTs:
Holographic QCD, LF QCD, Relativistic Confined Quark Model
- Future prospects for Nucleon Resonances
- Summary

Introduction

- Manifestation of composite structure of baryons - rich spectrum of resonances/excited states and their decay properties (e.g. electrocouplings)
- Light baryons: Mass region $1 - 2 \text{ GeV}$
- Experimental study: electromagnetic (e^- , γ) and strong (π , K , ...) beams
- Fundamental d.o.f. - quarks, gluons, sea quarks, meson cloud, molecular components ?
- Normally nucleon structure is studied in fixed-target DIS experiments (from pioneer SLAC exp to JLab, BNL exp) giving access to PDFs, FFs
 - Inclusive DIS: $e + p \rightarrow e' + X$
 - Semi-inclusive DIS (SIDIS): $e + p \rightarrow e' + X + H_1 + \dots + H_n$
- Excited baryons: JLab, ELSA, MAMI, GRAAL, SPring-8, ... via scattering with meson-nucleon final states

Introduction

- From theoretical point of view: QCD can not be applied
- Lattice QCD, QCD motivated approaches, Coupled-channel approaches/Reaction models provide the main tool for study of excited baryon structure
- QCD motivated approaches:
 - Light-Front QCD
 - QCD Sum Rules
 - ChPT
 - Large N_c
 - Schwinger-Dyson (SDE) and Bethe-Salpeter Equations (BSE)
 - Quark Models
 - AdS/QCD
- Coupled-Channel Approaches/Reaction Models:
 - BoGa (Bonn-Gatchina)
 - EBAC (Argon-Osaka)
 - JAW (Jülich-Athens-Washington)
 - JPAC (Joint Physics Analysis Center = Indiana-JLab-...)

Introduction

- Lattice QCD: improve of computing technologies, reduce of pion mass
- See talks David Richards, Raul Briceno
- Mass spectrum, Radiative transitions, ...
- Phys Rev D84 (2011) 074508, D85 (2012) 054016, D87 (2013) 054506, ...
- Lattice QCD ingredients
 - 1) Baryonic interpolating operators, 2) Running quark mass are used in QCD motivated approaches

Introduction

- Baryonic interpolating operators are constructed from product of three quark fields (quark interpolating currents) transforming as irreducible representation of $SU(3)_F$ for flavor $SU(4)_S$ for Dirac spins of quarks $O(3)_L$ for orbital angular momenta
- Covariant derivatives: to realize nontrivial orbital angular momenta
- $B = (\mathcal{F}_{\Sigma_F} \otimes \mathcal{S}_{\Sigma_S} \otimes \mathcal{D}_{\Sigma_D}) \{q_1 q_2 q_3\}$
- $\mathcal{F}, \mathcal{S}, \mathcal{D}$ are flavor, Dirac spin, spatial projection operators
- $\Sigma_F, \Sigma_S, \Sigma_D$ - symmetry combinations of flavor, spin, spatial coordinates
- For ground states (symmetric spatial w.f.) $B = (\mathcal{F}_{\Sigma_F} \otimes \mathcal{S}_{\Sigma_S}) \{q_1 q_2 q_3\}$
- Roper: Five-quark operators with quantum numbers of Roper resonance
- Based on combining positive-parity mesons with conventional nucleon interpolators like $\pi N, a_0 N, \sigma N$ interpolating fields

Introduction

- Baryon interpolating currents in EFT (QCD sum rules, relativistic quark models) complementing Lattice QCD

- Proton

$$\varepsilon^{abc} \gamma^\mu \gamma^5 d^a \left(u^b C \gamma_\mu u^c \right) \text{ (vector current)}$$

$$\varepsilon^{abc} \sigma^{\mu\nu} \gamma^5 d^a \left(u^b C \sigma_{\mu\nu} u^c \right) \text{ (tensor current)}$$

- Excited states

$$\varepsilon^{abc} \gamma^5 D^\mu(d^a) \left(u^b C \gamma_\mu u^c \right)$$

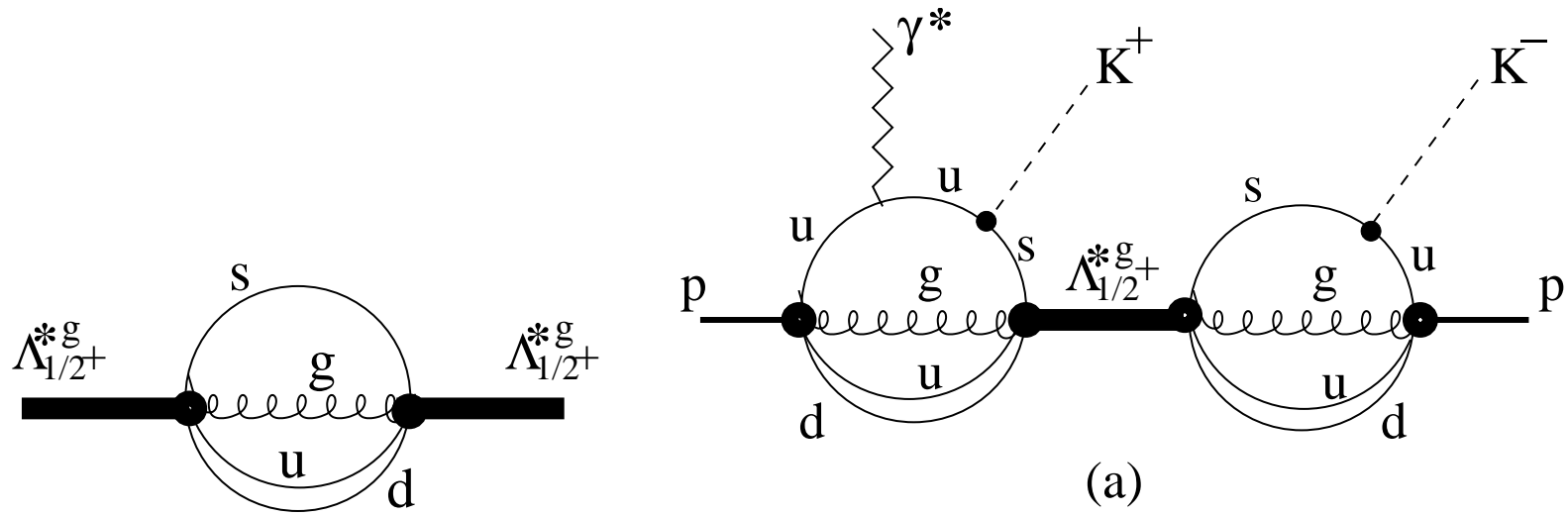
- Hybrids

$$\varepsilon^{abc} G_{\mu\nu}^{ad} \gamma^\mu q^d \left(q^b C \gamma^\nu q^c \right)$$

Here $G_{\mu\nu}^{ad}$ is stress tensor of gluon field

Introduction

- Proposal of Tübingen-Moscow-Dubna-Mainz group
“Study of hybrid mesons and baryons in relativistic confined quark model”
- Support of the CLAS12 and GlueX Collaborations at JLab



- Take into account next-to-leading order $qqqG$ Fock component in the nucleon
 $|p\rangle = \cos\theta|qqq\rangle + \sin\theta|qqqG\rangle$
- Test gluon content in nucleon/conventional baryons

Introduction

- Basic Equation for study of bound states in QFT
- Compositeness condition $Z_2 = 1 - g_H^2 \Sigma'_H(m_H^2) = 0$
- Introduced Salam, Weinberg (1962-1963)
- Equivalent to normalization of bound-state w.f. in BSE approach

$$1 = g_H^2 \Sigma'_H(m_H^2)$$

- Equivalent to Ward identity (WI) relating EM FF at $q^2 = 0$ and derivative of mass operator on mass shell

$$\underbrace{g_H^2 \partial \Sigma_H(p)/\partial p^\mu}_{\text{Ward Identity}} = \Lambda^\mu(p, p) = 2p^\mu F(0) = 2p^\mu \quad \text{for } F(0) = 1$$

$$g_H^2 \partial \Sigma(p)/\partial p^\mu = 2p^\mu g_H^2 \Sigma'(m_H^2) \longrightarrow g_H^2 \Sigma'(m_H^2) = 1$$

Introduction

- Running quark mass
- Initial scale μ : no hard-gluon or soft-gluon dressing
- SDE approach provide dressing of quark mass by soft-gluon configurations
- It is so-called **evolution to low scale**
- Be careful with dressing by hard gluons
- It is so-called **evolution to higher scale**
- Must be agreement with pQCD
- For resolution scales $\mu \sim E = 12$ GeV dressed quark is negligible
- Factorization theorem: observables are μ -independent.
- They are product of pQCD cross sections (perturbative objects) and PDFs (nonperturbative objects)
- μ evolution of one is compensated by evolution of the second
- PDFs are universal for specific hadron and extracted from data
- Good check of QCD motivated approaches calculating them

QCD Compositeness and Quark Counting Rules

QCD compositeness vs. VMD

Brodsky, Lebed, Lyubovitskij: hep-ph/1609.06635, appear in PLB

- Novel idea relevant for electrocouplings of baryon resonances
- QCD compositeness (vector mesons are bound states of quarks) leads to a nontrivial Q^2 dependence of vector meson - photon transition
- In Vector Meson Dominance Model (VMD) is constant $G_V(g^{\mu\nu}q^2 - q^\mu q^\nu)$
- Must have $1/\sqrt{Q^2}$ behavior at large Q^2
- Consider the pion
- In VMD: contact diagram 1, vector meson diagram gives $-Q^2/(M_V^2 + Q^2)$
- The sum is $M_V^2/(M_V^2 + Q^2)$ scales as M_V^2/Q^2
- Contact diagram is 1, resonance is $-1 + M_V^2/Q^2$
- In pQCD: contact diagram $1/Q^2$, vector meson diagram is subleading $1/Q^3$ because of falloff of the vector meson-photon form factor

QCD Compositeness and Quark Counting Rules

- New formula for electrocouplings of two hadrons with adjustable constituent content n_1 and n_2

$$\begin{aligned} F_{H_{n_1} H_{n_2}}(Q^2) &= \frac{\Gamma(\frac{n_1+n_2}{2}) \Gamma(\frac{n_1+n_2}{2} - 1)}{\sqrt{\Gamma(n_1 - 1)\Gamma(n_2 - 1)}} \frac{\Gamma(a + 1)}{\Gamma(a + 1 + \frac{n_1+n_2}{2} - 1)} \\ &\sim \frac{1}{a^{(n_1+n_2)/2-1}}, \end{aligned}$$

where $a = Q^2/(4\kappa^2)$.

For $n_1 = n_2 = n$ we get

$$F_{H_n} \sim \left(\frac{1}{Q^2}\right)^{n-1}$$

For $n_1 = n, n_2 = 0$ we get

$$F_{H_n} \sim \left(\frac{1}{Q^2}\right)^{(n-1)/2}$$

QCD Compositeness and Quark Counting Rules

- In particular, the scaling of the form factor corresponding to $\gamma^* \rightarrow Z_c^+ + \pi^-$ is

$$F_{Z_c^+ \pi^-} \sim \frac{1}{Q^4}$$

in case of tetraquark structure of Z_c state, and

$$F_{Z_c^+ \pi^-} \sim \frac{1}{Q^2}$$

in the case when Z_c^+ is a system of two tightly bound diquarks.

For $\gamma^* \rightarrow Z_c^+ + Z_c^-$,

$$F_{Z_c^+ Z_c^-} \sim \frac{1}{Q^6}$$

in case of a Z_c state with tetraquark structure, and

$$F_{Z_c^+ Z_c^-} \sim \frac{1}{Q^2}$$

in case when Z_c^+ is a system of two tightly bound diquarks (Brodsky and Lebed)

Baryons in AdS/QCD

- $S_\psi = \int d^d x dz \sqrt{g} \bar{\Psi}(x, z) \left(\not{D} - \mu - \varphi(z)/R \right) \Psi(x, z)$

- Field decomposition (left/right) and KK expansion

$$\Psi(x, z) = \Psi_L(x, z) + \Psi_R(x, z) \quad \Psi_{L/R} = \frac{1 \mp \gamma^5}{2} \Psi$$

$$\Psi_{L/R}(x, z) = \sum_n \Psi_{L/R}^n(x) F_{L/R}^n(z)$$

- EOM

$$\left[-\partial_z^2 + \kappa^4 z^2 + 2\kappa^2 \left(\mu R \mp \frac{1}{2} \right) + \frac{\mu R(\mu R \pm 1)}{z^2} \right] F_{L/R}^n(z) = M_n^2 F_{L/R}^n(z)$$

Solutions (for $d = 4$ and $\mu R = L + 3/2$)

- Bulk profiles

$$F_L^n(z) = \sqrt{\frac{2\Gamma(n+1)}{\Gamma(n+L+3)}} \kappa^{L+3} z^{L+9/2} e^{-\kappa^2 z^2/2} L_n^{L+2}(\kappa^2 z^2)$$

$$F_R^n(z) = \sqrt{\frac{2\Gamma(n+1)}{\Gamma(n+L+2)}} \kappa^{L+2} z^{L+7/2} e^{-\kappa^2 z^2/2} L_n^{L+1}(\kappa^2 z^2)$$

- Mass spectrum: $M_{nL}^2 = 4\kappa^2 (n + L + 2)$

Baryons in AdS/QCD

- Scattering problem for AdS field gives information about propagation of external field from z to the boundary $z = 0$ — bulk-to-boundary propagator $\Phi_{\text{ext}}(q, z)$
[Fourier-transform of AdS field $\Phi_{\text{ext}}(x, z)$]:

$$\Phi_{\text{ext}}(q, z) = \int d^d x e^{-iqx} \Phi_{\text{ext}}(x, z)$$

- Vector field as example

$$\partial_z \left(\frac{e^{-\varphi(z)}}{z} \partial_z V(q, z) \right) + q^2 \frac{e^{-\varphi(z)}}{z} V(q, z) = 0.$$

$$V(Q, z) = \Gamma\left(1 + \frac{Q^2}{4\kappa^2}\right) U\left(\frac{Q^2}{4\kappa^2}, 0, \kappa^2 z^2\right)$$

Consistent with GI, fulfills UV and IR boundary conditions :

$$V(Q, 0) = 1, \quad V(Q, \infty) = 0$$

- Hadron form factors

$$F_\tau(Q^2) = \langle \phi_\tau | \hat{V}(Q) | \phi_\tau \rangle = \int_0^\infty dz \phi_\tau^2(z) V(Q, z) = \frac{\Gamma(\tau) \Gamma(a+1)}{\Gamma(a+\tau)}$$

is implemented by a nontrivial dependence of AdS fields on 5-th coordinate

Introduction

- Power scaling at large Q^2

$$F_\tau(Q^2) \sim \frac{1}{(Q^2)^{\tau-1}}$$

Quark counting rules: Matveev-Muradyan-Tavhelidze-Brodsky-Farrar 1973

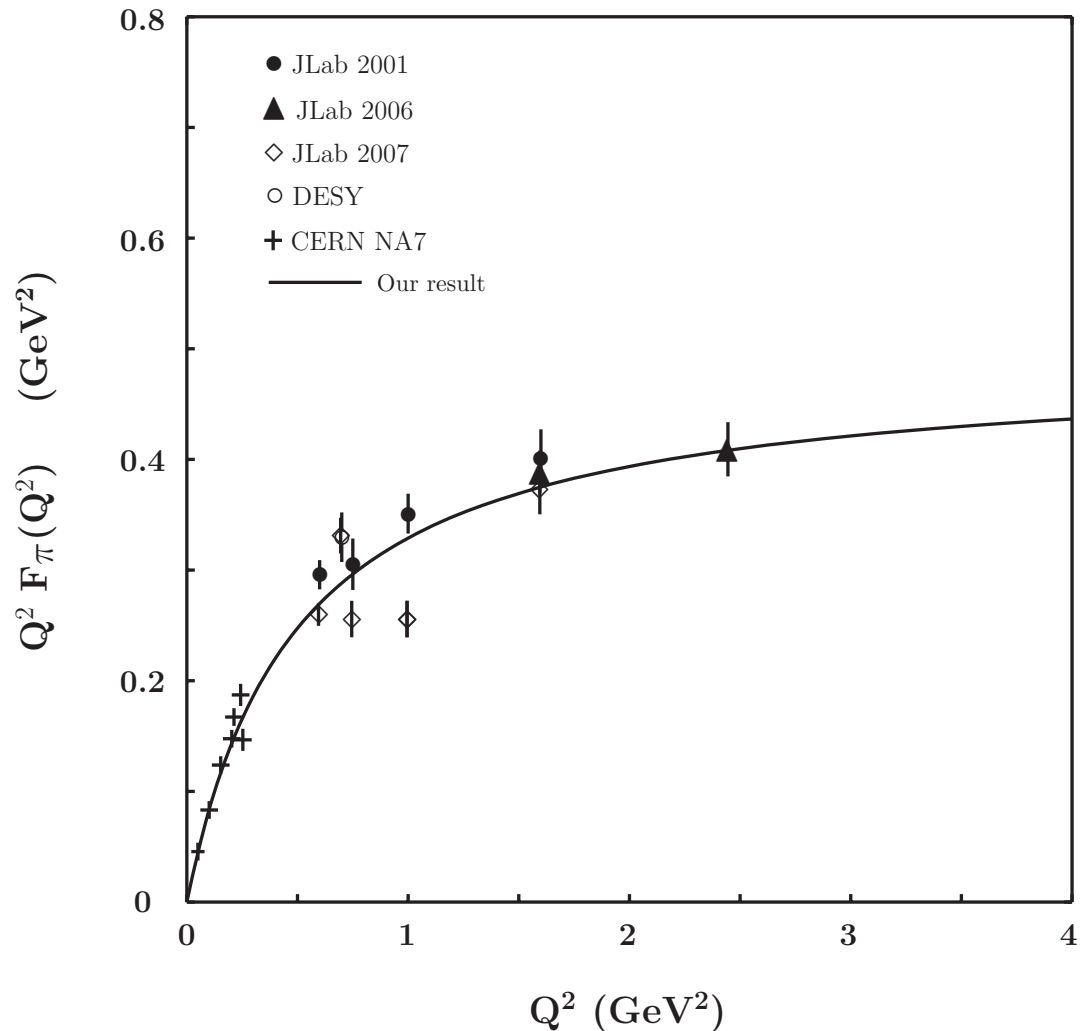
$$\text{Pion} : \frac{1}{Q^2}$$

$$\text{Nucleon(Dirac)} : \frac{1}{Q^4}$$

$$\text{Nucleon(Pauli)} : \frac{1}{Q^6}$$

$$\text{Deuteron(Charge)} : \frac{1}{Q^{10}}$$

Mesons: pion form factor



LFWFs motivated by holographic QCD

- Matching matrix elements (e.g. form factors) in HQCD and LF QCD
- Drell-Yan-West formula

$$F_\tau(Q^2) = \int_0^1 dx \int \frac{d^2 \mathbf{k}_\perp}{16\pi^3} \psi_\tau^\dagger(x, \mathbf{k}'_\perp) \psi_\tau(x, \mathbf{k}_\perp),$$

where $\psi(x, \mathbf{k}_\perp) \equiv \psi(x, \mathbf{k}_\perp; \mu_0)$, $\mathbf{k}'_\perp = \mathbf{k}_\perp + (1-x)\mathbf{q}_\perp$, and $Q^2 = \mathbf{q}_\perp^2$

- HQCD

$$F_\tau(Q^2) = \int_0^\infty dz V(Q, z) \varphi_\tau^2(z) = \frac{\Gamma(\frac{Q^2}{4\kappa^2} + 1) \Gamma(\tau)}{\Gamma(\frac{Q^2}{4\kappa^2} + \tau)}.$$

- Result for effective LFWF at the initial scale μ_0

$$\psi_\tau(x, \mathbf{k}_\perp) = \sqrt{\tau - 1} \frac{4\pi}{\kappa} \sqrt{\log(1/x)} (1-x)^{\frac{\tau-4}{2}} \exp\left[-\frac{\mathbf{k}_\perp^2}{2\kappa^2} \frac{\log(1/x)}{(1-x)^2}\right]$$

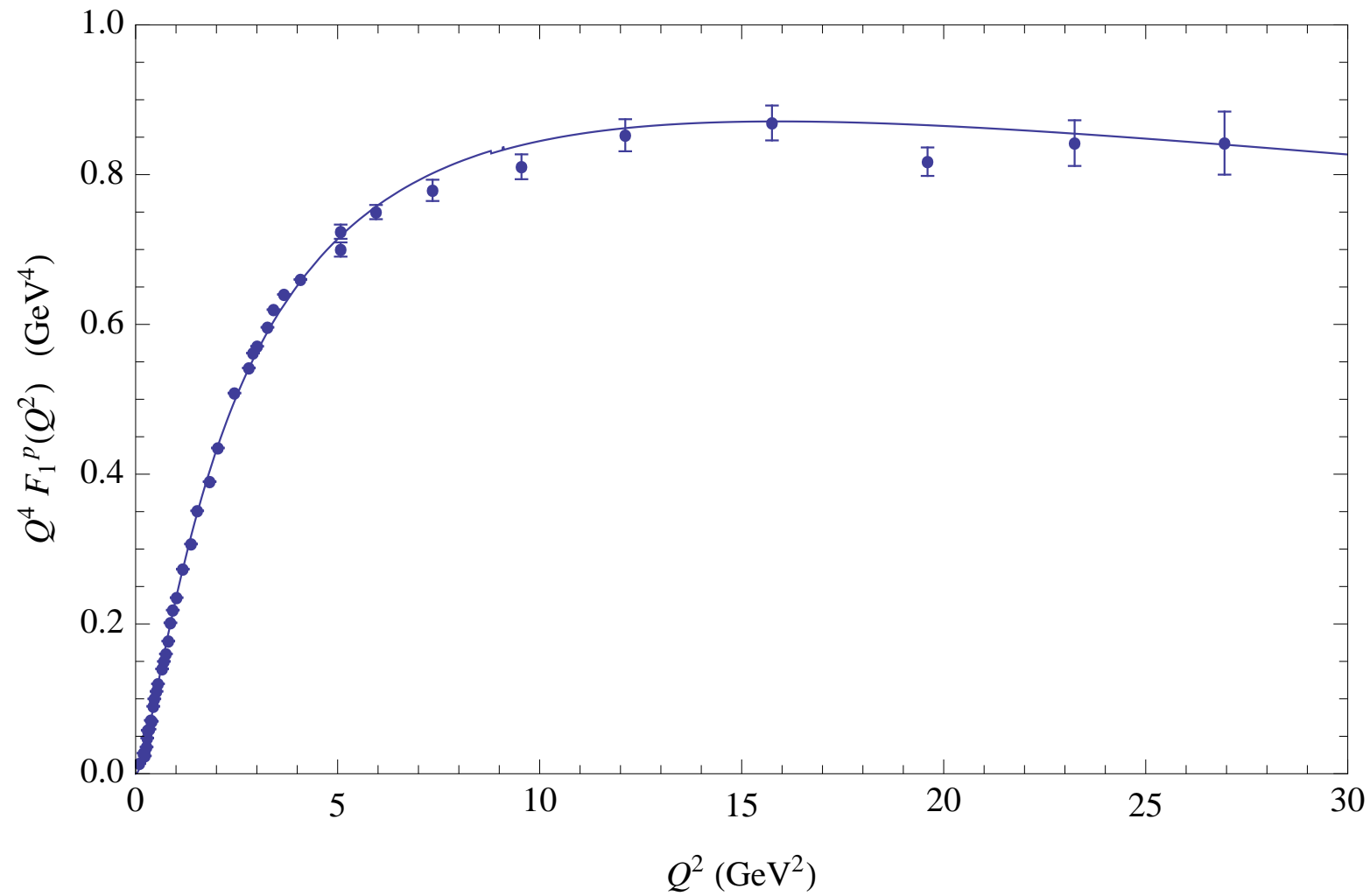
- At large x PDFs have different scaling: $q_\pi(x) \sim 1$, $q_N(x) \sim 1 - x$

Nucleon Properties

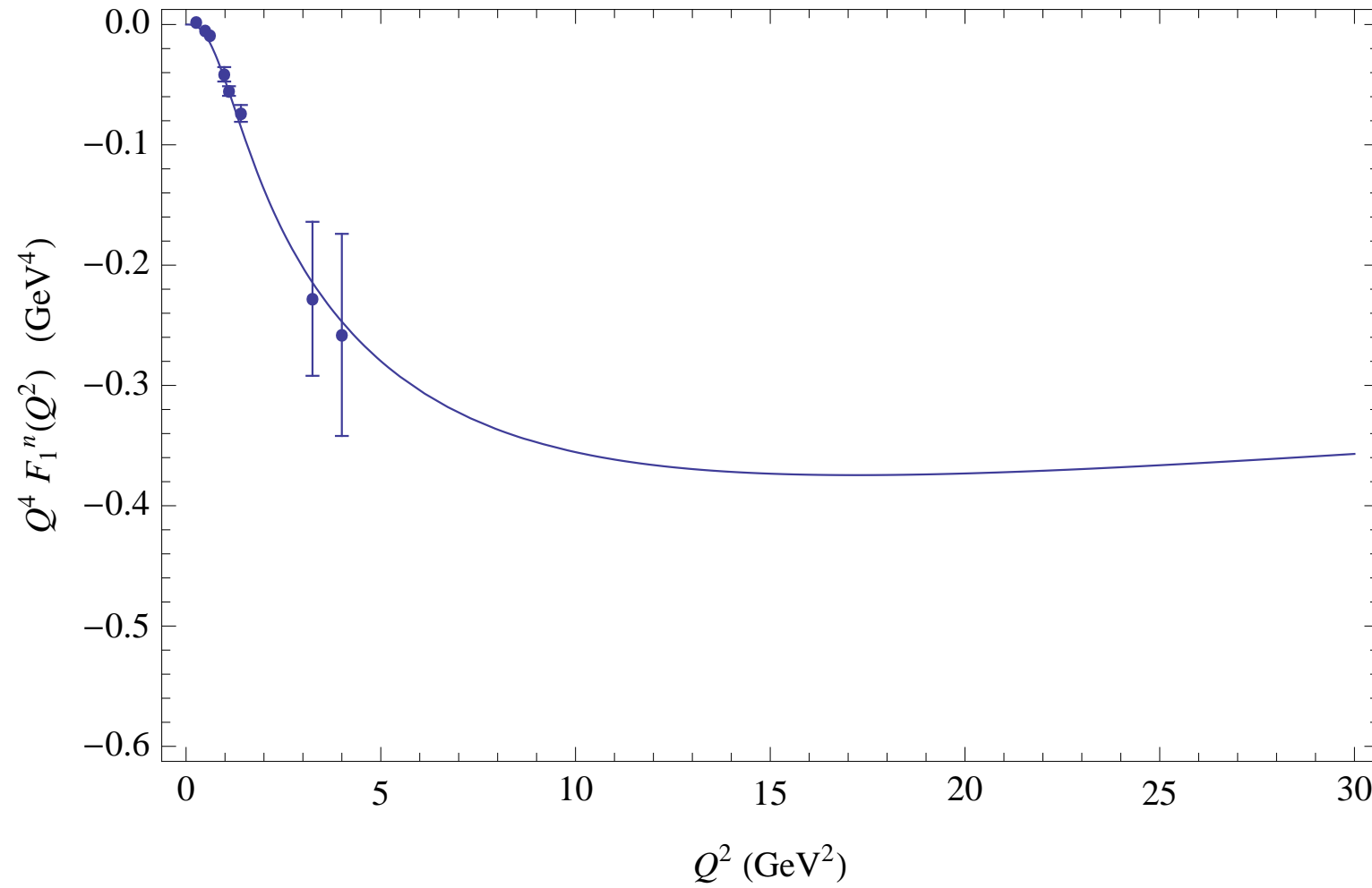
Mass and electromagnetic properties of nucleons

Quantity	Our results	Data
m_p (GeV)	0.93827	0.93827
μ_p (in n.m.)	2.793	2.793
μ_n (in n.m.)	-1.913	-1.913
r_E^p (fm)	0.840	0.8768 ± 0.0069
$\langle r_E^2 \rangle^n$ (fm 2)	-0.117	-0.1161 ± 0.0022
r_M^p (fm)	0.785	$0.777 \pm 0.013 \pm 0.010$
r_M^n (fm)	0.792	$0.862^{+0.009}_{-0.008}$
r_A (fm)	0.667	0.67 ± 0.01

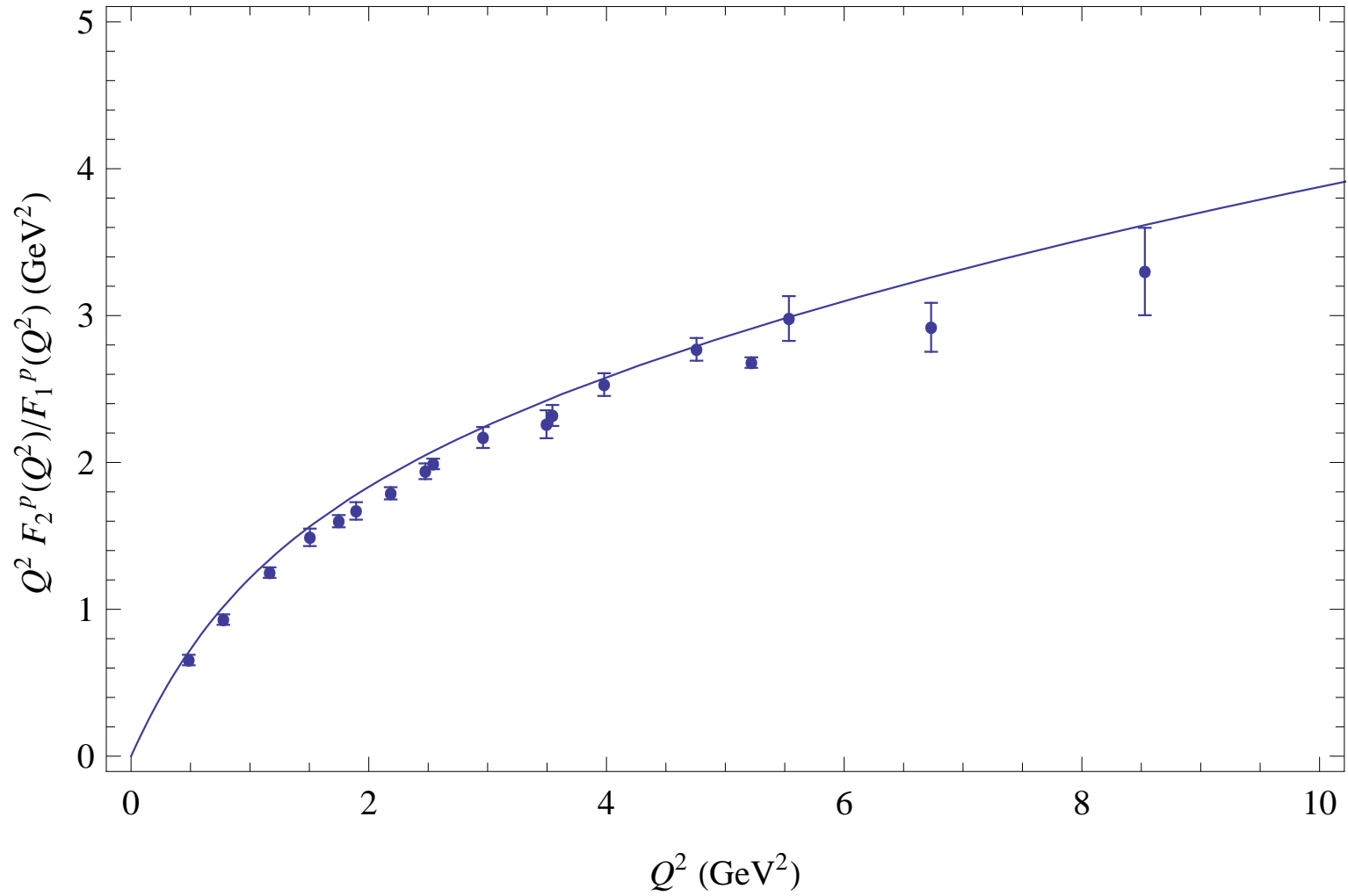
Nucleon as quark-scalar diquark in LFQM



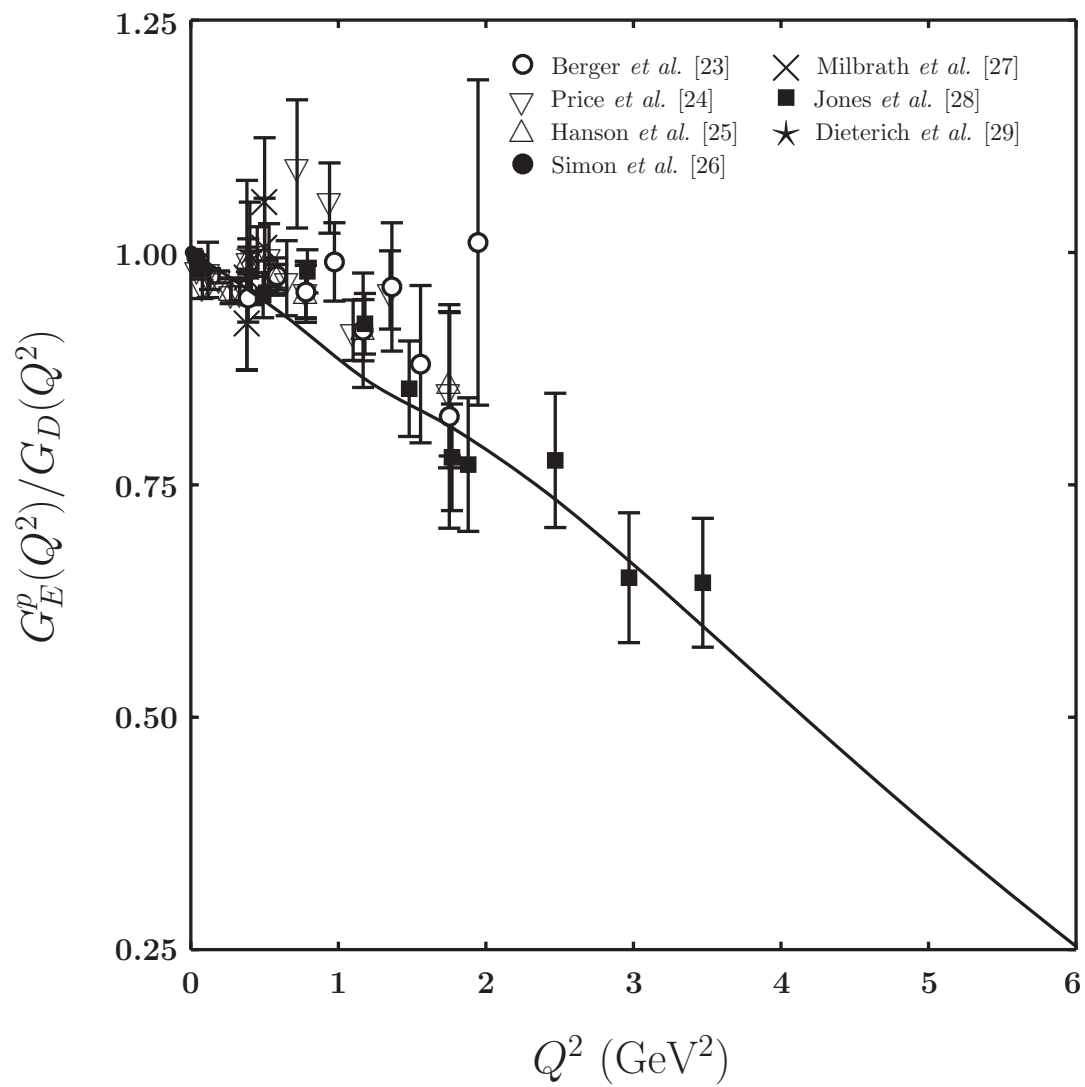
Nucleon as quark-scalar diquark in LFQM



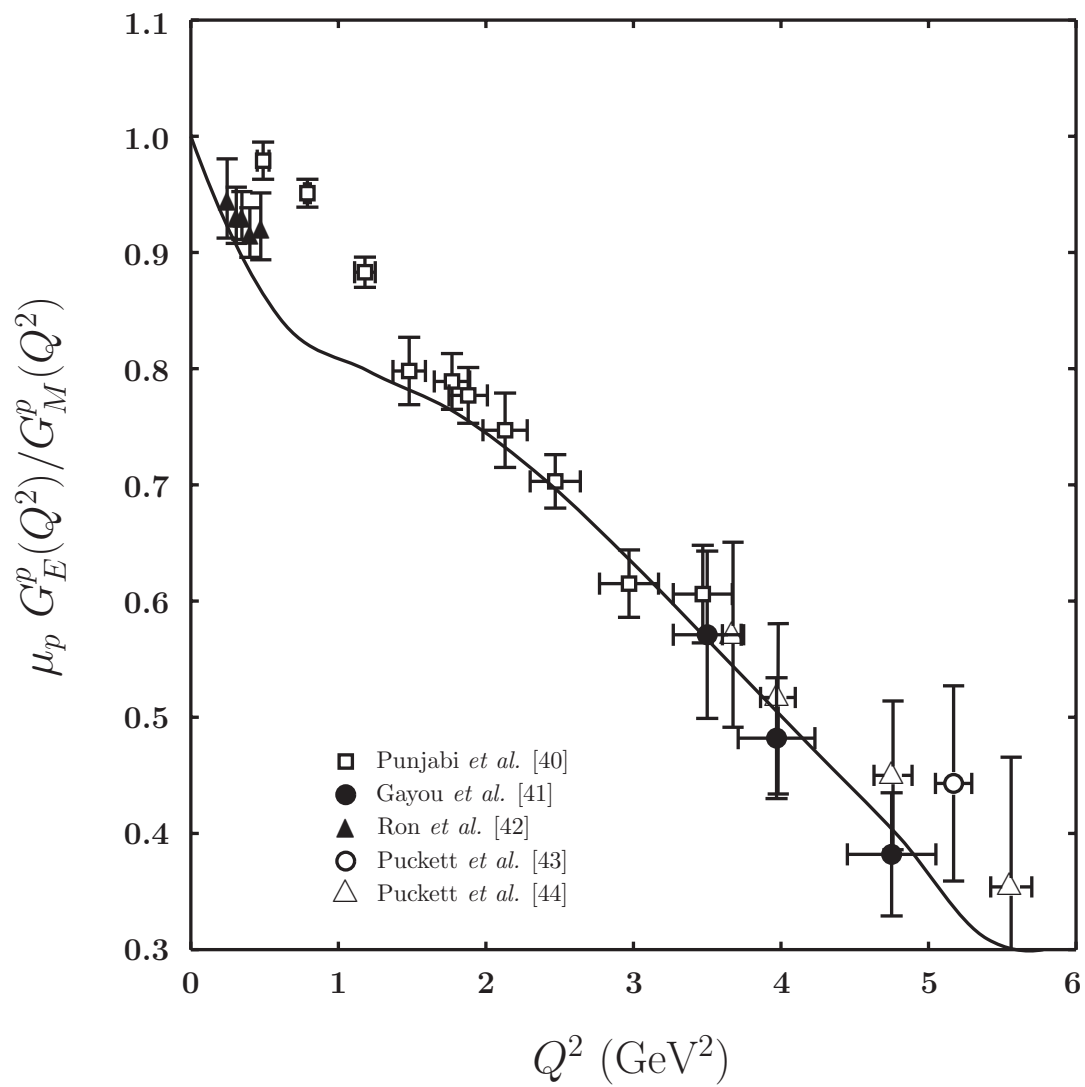
Nucleon as quark-scalar diquark in LFQM



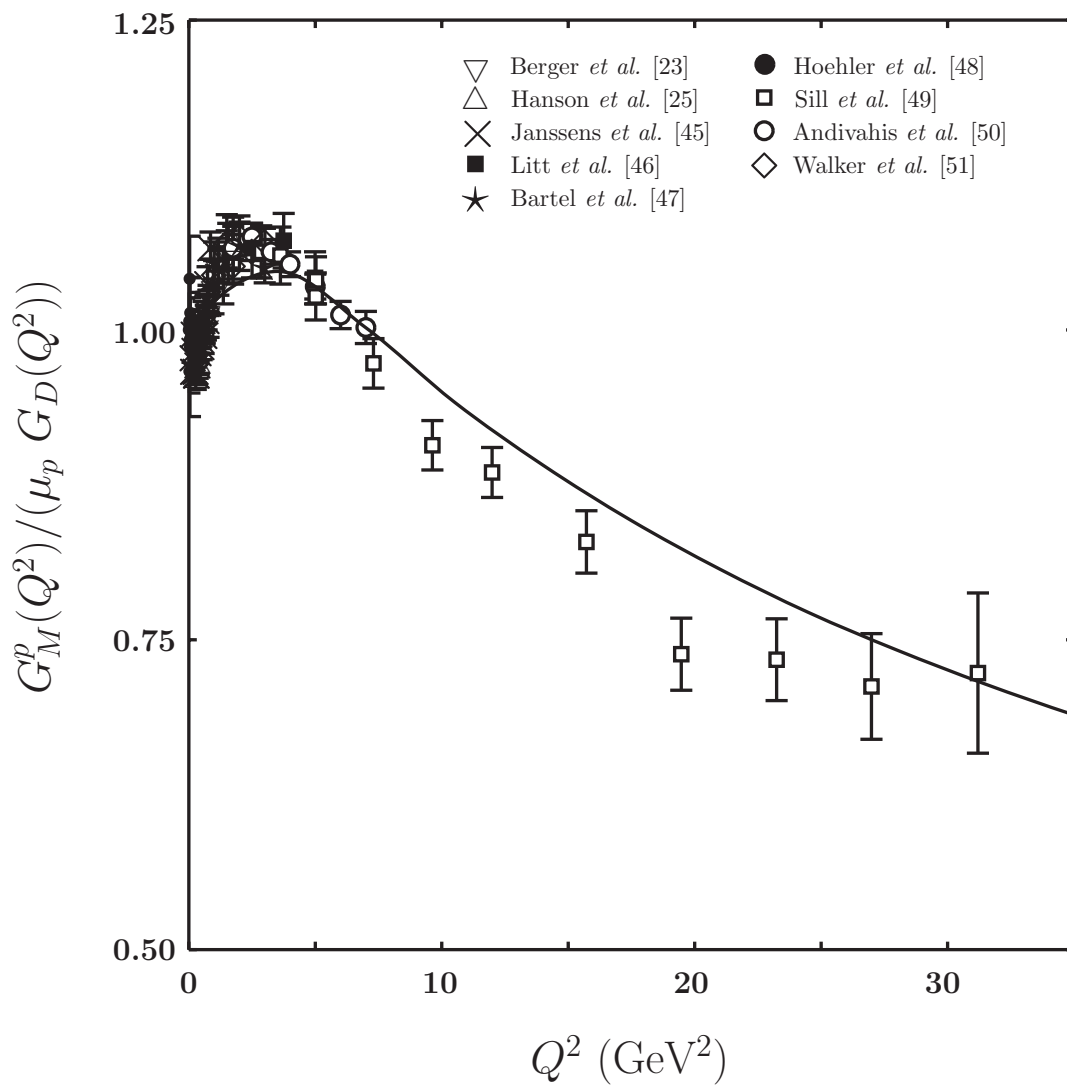
Nucleon as quark-scalar diquark in LFQM



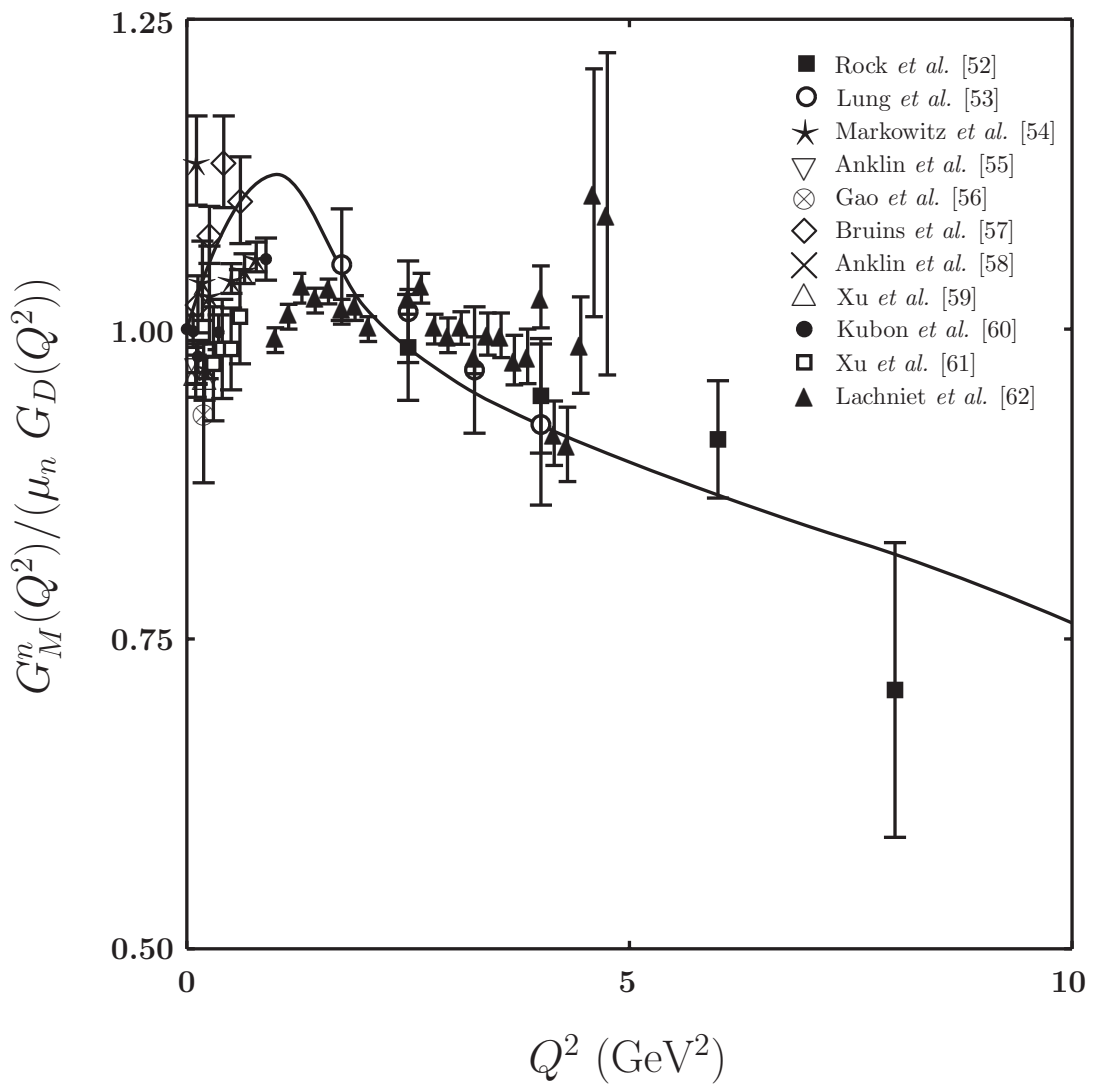
Nucleon as quark-scalar diquark in LFQM



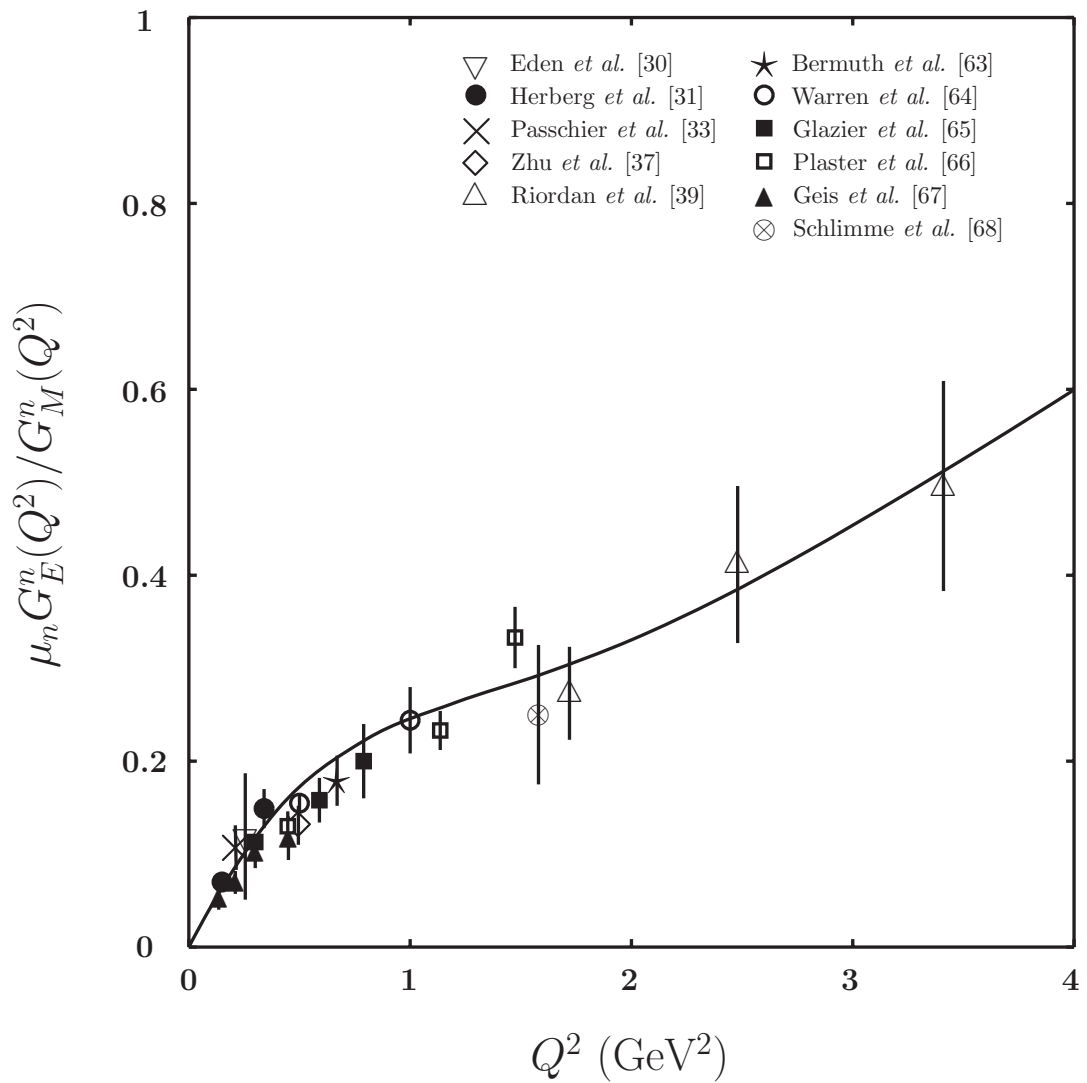
Nucleon as quark-scalar diquark in LFQM



Nucleon as quark-scalar diquark in LFQM



Nucleon as quark-scalar diquark in LFQM



Roper resonance $N(1440)$

- Put $n = 1$ and get solutions dual to Roper:

$$M_{\mathcal{R}} \simeq 1440 \text{ MeV}$$

- $N \rightarrow R + \gamma$ transition

$$M^\mu = \bar{u}_{\mathcal{R}} \left[\gamma_\perp^\mu F_1(q^2) + i\sigma^{\mu\nu} \frac{q_\nu}{M_{\mathcal{R}}} F_2(q^2) \right] u_N, \quad \gamma_\perp^\mu = \gamma^\mu - q^\mu \frac{\not{q}}{q^2}$$

- Helicity amplitudes

$$\begin{aligned} H_{\pm \frac{1}{2}0} &= \sqrt{\frac{Q_-}{Q^2}} \left(F_1 M_+ - F_2 \frac{Q^2}{M_{\mathcal{R}}} \right) \\ H_{\pm \frac{1}{2}\pm 1} &= -\sqrt{2Q_-} \left(F_1 + F_2 \frac{M_+}{M_{\mathcal{R}}} \right) \end{aligned}$$

- Alternative set [Weber, Capstick, Copley et al]

$$A_{1/2} = -b H_{\frac{1}{2}1}, \quad S_{1/2} = b \frac{|\mathbf{p}|}{\sqrt{Q^2}} H_{\frac{1}{2}0},$$

$$Q_\pm = M_\pm^2 + Q^2, \quad M_\pm = M_{\mathcal{R}} \pm M_N, \quad b = \sqrt{\frac{\pi\alpha}{2EM_{\mathcal{R}}M_N}}$$

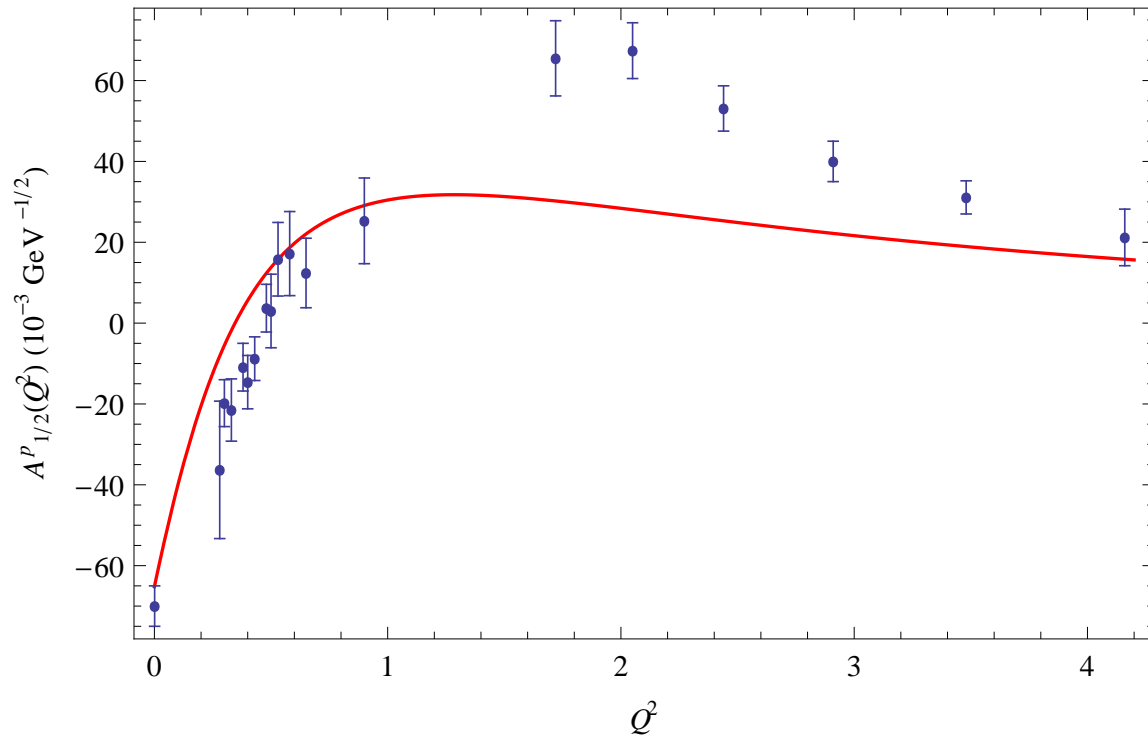
Roper resonance $N(1440)$

Helicity amplitudes $A_{1/2}^N(0)$, $S_{1/2}^N(0)$

Quantity	Our results	Data
$A_{1/2}^p(0) (\text{GeV}^{-1/2})$	-0.065	-0.065 ± 0.004
$A_{1/2}^n(0) (\text{GeV}^{-1/2})$	0.040	0.040 ± 0.010
$S_{1/2}^p(0) (\text{GeV}^{-1/2})$	0.040	
$S_{1/2}^n(0) (\text{GeV}^{-1/2})$	-0.040	

Roper resonance $N(1440)$

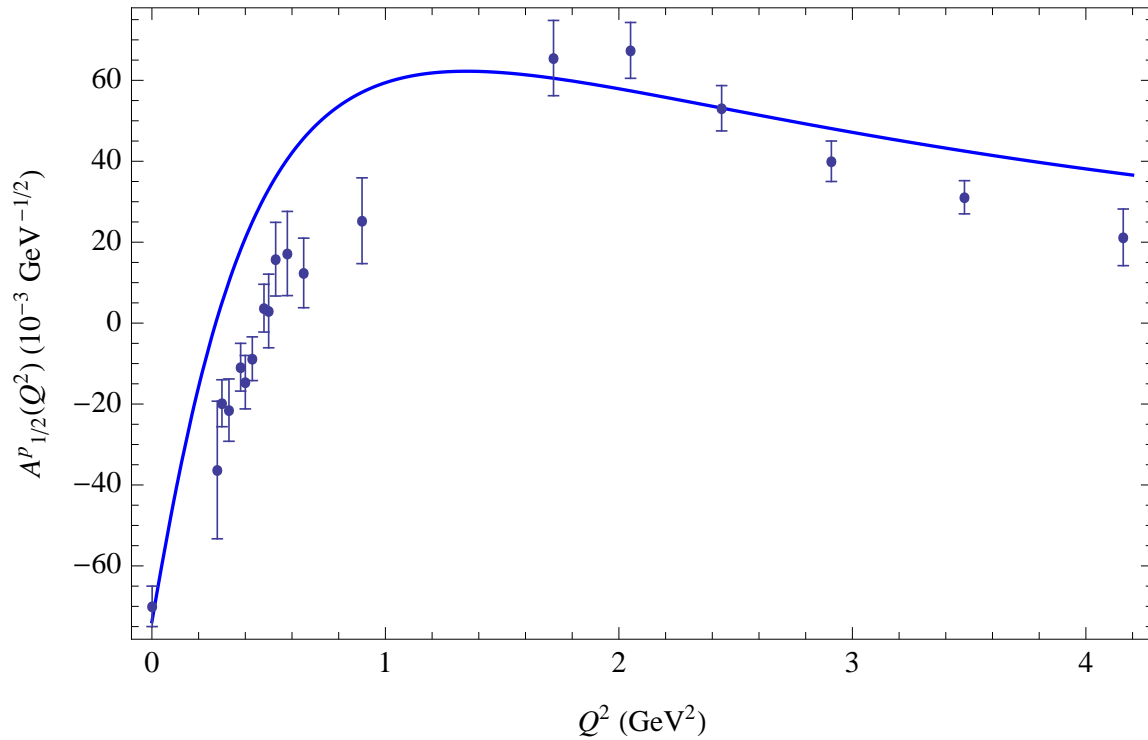
Helicity amplitude $A_{1/2}^p(Q^2)$



Data: CLAS Coll at JLab, Mokeev et al, PRC86 (2012) 035203

Roper resonance $N(1440)$

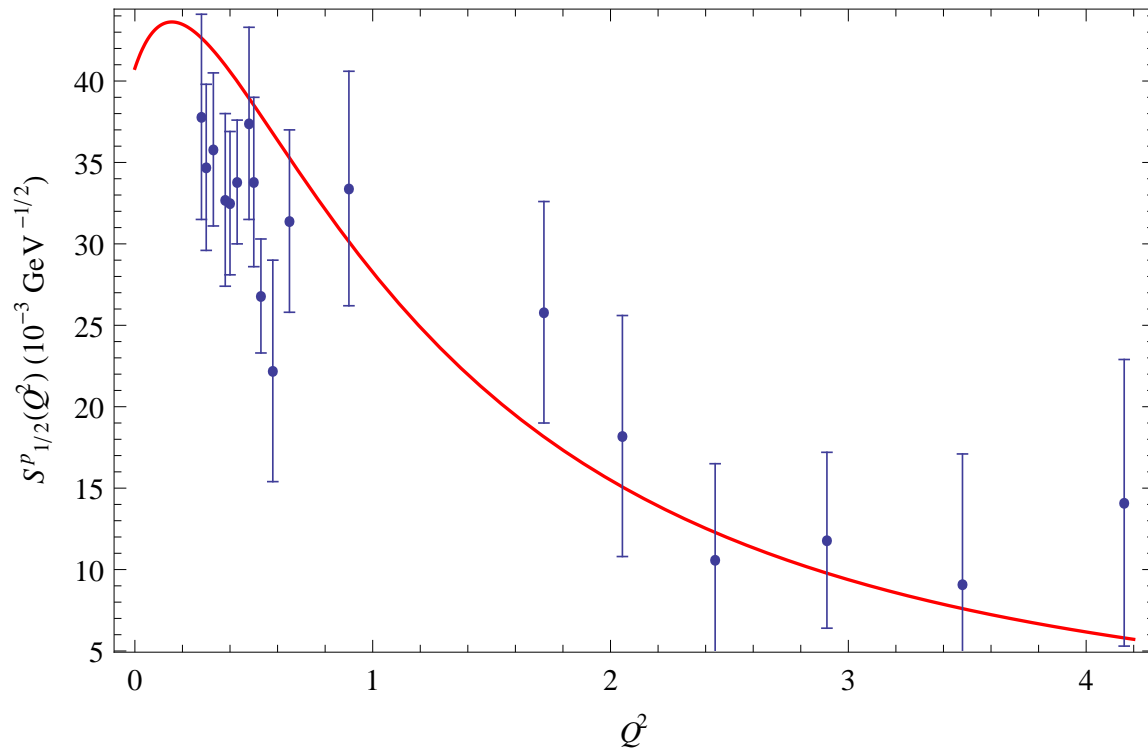
Helicity amplitude $A_{1/2}^p(Q^2)$



Data: CLAS Coll at JLab, Mokeev et al, PRC86 (2012) 035203

Roper resonance $N(1440)$

Helicity amplitude $S_{1/2}^p(Q^2)$



Data: CLAS Coll at JLab, Mokeev et al, PRC86 (2012) 035203

Deuteron

- Effective action in terms of AdS fields $d^M(x, z)$ and $V^M(x, z)$
- $d^M(x, z)$ – dual to Fock component contributing to deuteron with twist $\tau = 6$
- $V^M(x, z)$ – dual to the electromagnetic field

$$\begin{aligned} S = & \int d^4x dz e^{-\varphi(z)} \left[-\frac{1}{4} F_{MN}(x, z) F^{MN}(x, z) - D^M d_N^\dagger(x, z) D_M d^N(x, z) \right. \\ & - ic_2(z) F^{MN}(x, z) d_M^\dagger(x, z) d_N(x, z) \\ & + \frac{c_3(z)}{4M_d^2} \partial^M F^{NK}(x, z) \left(-d_M^\dagger(x, z) \overset{\leftrightarrow}{D}_K d_N(x, z) + \text{H.c.} \right) \\ & \left. + d_M^\dagger(x, z) \left(\mu^2 + U(z) \right) d^M(x, z) \right] \end{aligned}$$

Deuteron

- $F^{MN} = \partial^M V^N - \partial^N V^M$ - stress tensor of vector field

$D^M = \partial^M - ieV^M(x, z)$ - covariant derivative

$\mu^2 R^2 = (\Delta - 1)(\Delta - 3)$ - five-dimensional mass

$\Delta = 6 + L$ is the dimension of $d^M(x, z)$

L is the maximum value orbital angular momentum

$U(z) = U_0 \varphi(z)/R^2$ is the confinement potential

U_0 is constant fixed the deuteron mass.

Use axial gauge for both vector fields $d^z(x, z) = 0$ and $V^z(x, z) = 0$

Deuteron

- First perform Kaluza-Klein (KK) decomposition for vector AdS field dual to deuteron

$$d^\mu(x, z) = \exp \left[\frac{\varphi(z) - A(z)}{2} \right] \sum_n d_n^\mu(x) \Phi_n(z),$$

$d_n^\mu(x)$ is the tower of the KK fields dual to the deuteron fields with radial quantum number n and twist-dimension $\tau = 6$, and $\Phi_n(z)$ are their bulk profiles.

Then we derive the Schrödinger-type equation of motion for the bulk profile

$$\left[-\frac{d^2}{dz^2} + \frac{4(L+4)^2 - 1}{4z^2} + \kappa^4 z^2 + \kappa^2 U_0 \right] \Phi_n(z) = M_{d,n}^2 \Phi_n(z).$$

Deuteron

- The analytical solutions of this EOM read

$$\Phi_n(z) = \sqrt{\frac{2n!}{(n + L + 4)!}} \kappa^{L+5} z^{L+9/2} e^{-\kappa^2 z^2/2} L_n^{L+4}(\kappa^2 z^2),$$
$$M_{d,n}^2 = 4\kappa^2 \left[n + \frac{L+5}{2} + \frac{U_0}{4} \right],$$

where $L_n^m(x)$ are the generalized Laguerre polynomials.

- Restricting to the ground state ($n = 0, L = 0$) we get $M_d = 2\kappa \sqrt{\frac{5}{2} + \frac{U_0}{4}}$
- Using central value for deuteron mass $M_d = 1.875613 \text{ GeV}$ and $\kappa = 190 \text{ MeV}$ (fitted from data on electromagnetic deuteron form factors), we fix $U_0 = 87.4494$.

Deuteron

- We can compare this value for the deuteron scale parameter to the analogous one of κ_N defining the nucleon properties - mass and electromagnetic form factors. In description of nucleon case we fixed the value to $\kappa_N \simeq 380$ MeV, which is 2 times bigger than the deuteron scale parameter κ .
- Difference between the nucleon and deuteron scale parameters can be related to the change of size of the hadronic systems - the deuteron as a two-nucleon bound state is 2 times larger than the nucleon.

Deuteron

- The gauge-invariant matrix element describing the interaction of the deuteron with the external vector field (dual to the electromagnetic field) reads

$$\begin{aligned} M_{\text{inv}}^{\mu}(p, p') &= - \left(G_1(Q^2) \epsilon^*(p') \cdot \epsilon(p) - \frac{G_3(Q^2)}{2M_d^2} \epsilon^*(p') \cdot q \epsilon(p) \cdot q \right) (p + p')^{\mu} \\ &\quad - G_2(Q^2) \left(\epsilon^{\mu}(p) \epsilon^*(p') \cdot q - \epsilon^{*\mu}(p') \epsilon(p) \cdot q \right) \end{aligned}$$

where $\epsilon(\epsilon^*)$ and $p(p')$ are the polarization and four-momentum of the initial (final) deuteron, and $q = p' - p$ is the momentum transfer.

Deuteron

- Three EM form factors $G_{1,2,3}$ of the deuteron are related to the charge G_C , quadrupole G_Q and magnetic G_M form factors by
- Expressions for the form factors

$$G_C = G_1 + \frac{2}{3}\tau_d G_Q, \quad G_M = G_2, \quad G_Q = G_1 - G_2 + (1 + \tau_d)G_3, \quad \tau_d = \frac{Q^2}{4M_d^2}$$

These form factors are normalized at zero recoil as

$$G_C(0) = 1, \quad G_Q(0) = M_d^2 Q_d = 25.83, \quad G_M(0) = \frac{M_d}{M_N} \mu_d = 1.714$$

- $Q_d = 7.3424 \text{ GeV}^{-2}$ and $\mu_d = 0.8574$ – quadrupole and magnetic moments of the deuteron.

Deuteron

- Structure functions

$$\begin{aligned} A(Q^2) &= G_C^2(Q^2) + \frac{2}{3}\tau_d G_M^2(Q^2) + \frac{8}{9}\tau_d^2 G_Q^2(Q^2), \\ B(Q^2) &= \frac{4}{3}\tau_d(1 + \tau_d)G_M^2(Q^2). \end{aligned}$$

- Scaling at large Q^2 (Brodsky et al., Carlson et al.)

Leading : $\sqrt{A(Q^2)} \sim \sqrt{B(Q^2)} \sim G_C(Q^2) \sim 1/Q^{10}$

Subleading : $G_M(Q^2) \sim G_Q(Q^2) \sim 1/Q^{12}$

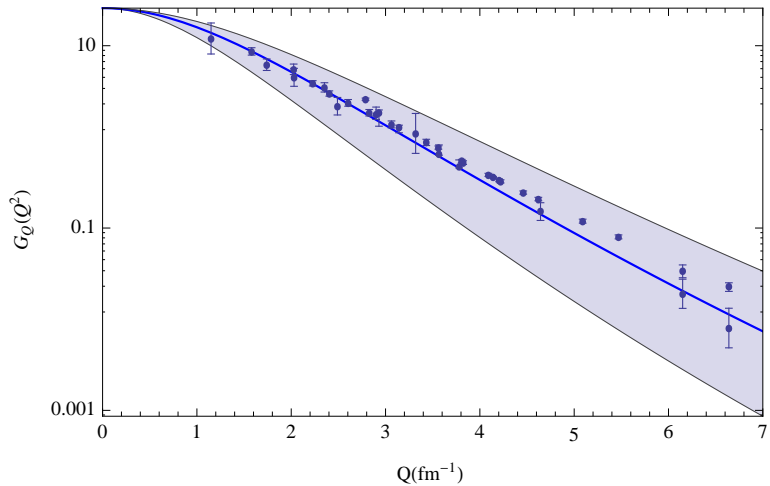
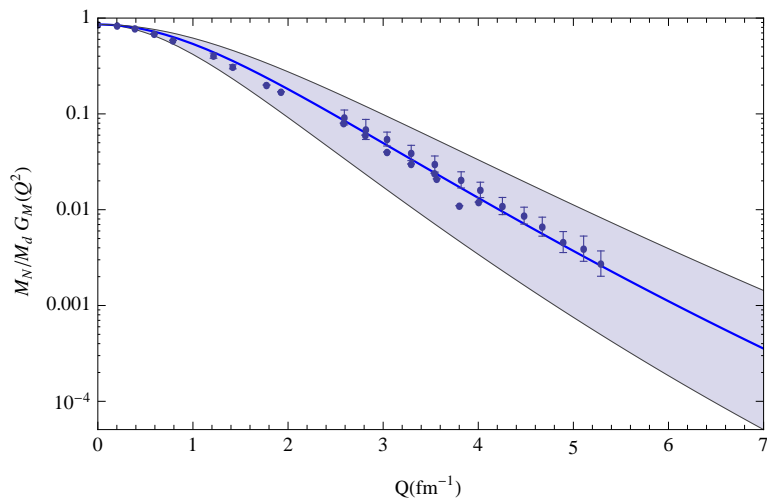
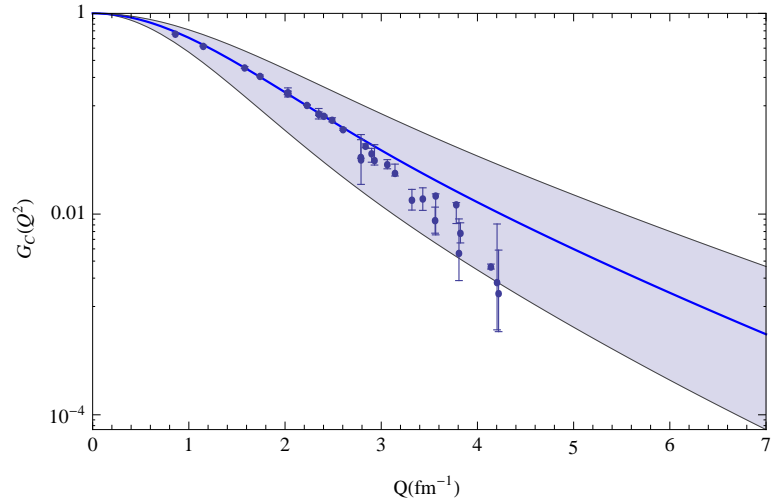
It fixes the z dependence of $c_2(z)$ and $c_3(z)$

$$\begin{aligned} c_2(z) &= \frac{M_d}{30M_N} \mu_d \kappa^2 z^2 \\ c_3(z) &= \left(M_d^2 Q_d - 1 + \frac{M_d}{30M_N} \mu_d \right) \kappa^2 z^2 \end{aligned}$$

Deuteron

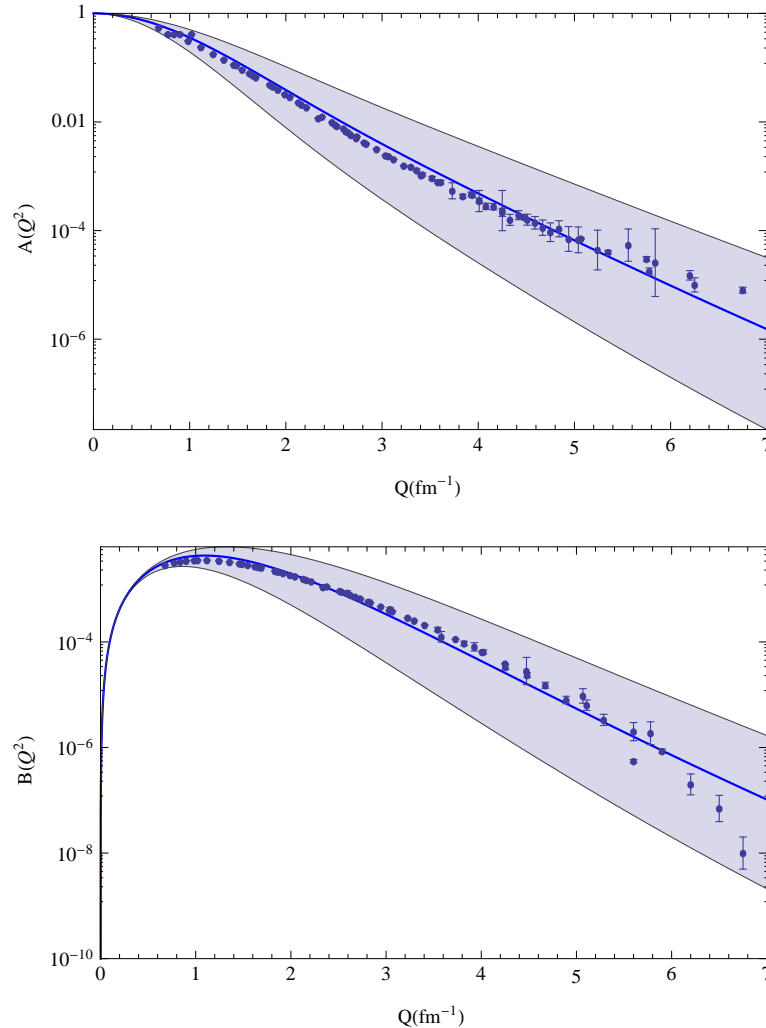
- Numerical results for the charge $G_C(Q^2)$, quadrupole $G_Q(Q^2)$ and magnetic $G_M(Q^2)$ FF
- Shaded band corresponds to values of κ in range of $150 \text{ MeV} < \kappa < 250 \text{ MeV}$.
- Increase of the parameter κ leads to an enhancement of the form factors.
- The best description of the data on the deuteron form factors is obtained for $\kappa = 190 \text{ MeV}$ and is shown by the solid line.

Deuteron



Deuteron form factors

Deuteron



Structure Functions $A(Q^2)$ and $B(Q^2)$

Deuteron

Charge radius

$$r_C = (-6G'_C(0))^{1/2} = 1.85 \text{ fm}$$

Data: $r_C = 2.13 \pm 0.01 \text{ fm}$

Magnetic radius $r_M = (-6G'_M(0)/G_M(0))^{1/2} = 2.29 \text{ fm}$

Data $r_M = 1.90 \pm 0.14 \text{ fm}$.

Tetraquarks

- N_c QCD: Mesons $q\bar{q}$ and under $SU(N_c)$ \bar{q}^a transforms similar to

$$\epsilon^{a a_1 \dots a_{N_c-1}} \underbrace{q_{a_1} \dots q_{N_c-1}}_{N_c-1}$$
- Baryons $\epsilon_{a_1 \dots a_{N_c}} \underbrace{q^{a_1} \dots q^{N_c}}_{N_c}$

$$\epsilon_{a_1 \dots a_{N_c-1} a} \epsilon_{b_1 \dots b_{N_c-1} a} \prod_{a_i, b_i=1}^{N_c-1} \underbrace{q^{a_i} \dots q^{b_i}}_{N_c-1}$$
 and q transforms as $\underbrace{\bar{q} \dots \bar{q}}_{N_c-1}$
- Multiquarks $\underbrace{q \dots q}_{N_c-1} \underbrace{\bar{q} \dots \bar{q}}_{N_c-1}$
- Limit to real QCD: $N_c = 3 \rightarrow$ Tetraquarks $qq\bar{q}\bar{q}$
- Equation of motion from mesons case by rescaling $\tau \rightarrow \tau + 2$
- Solutions: $\phi_{nL}(z) = \sqrt{\frac{2\Gamma(n+1)}{\Gamma(n+L+3)}} \kappa^{L+3} z^{L+17/2} e^{-\kappa^2 z^2/2} L_n^{L+2}(\kappa^2 z^2)$
- $M_{nJL}^2 = 4\kappa^2 \left(n + \frac{L+J}{2} + 1 \right)$

Tetraquarks

- Agreement with the COMPASS Coll. at SPS (CERN) for $a_1(1414)$ with spin-parity $J^{PC} = 1^{++}$ discovered in 2015
- Put $n = 0, L = 1, J = 1$ and get $M_{a_1}^2 = 8\kappa^2$ or $M_{a_1} = 2\kappa\sqrt{2}$
- Using $\kappa = 0.5 \text{ GeV}$ get $M_{a_1} = \sqrt{2} \simeq 1.414 \text{ GeV}$
- Comparison with Stan Brodsky - Guy Teramond
- Brodsky-Teramond (superconformal case) $M_{nJL}^2 = 4\kappa^2 \left(n + L + \frac{S}{2} + 1 \right)$
- Our $M_{nJL}^2 = 4\kappa^2 \left(n + \frac{L+J}{2} + 1 \right)$
- Merge at $J = L + S$, which is true when all three decouple
- It is not the case for $a_1(1414)$ for which $J = L = S = 1$

Nucleon as quark-scalar diquark in LFQM

$$\begin{aligned}
 \psi_{+q}^+(x, \mathbf{k}_\perp) &= \varphi_q^{(1)}(x, \mathbf{k}_\perp), \\
 \psi_{-q}^+(x, \mathbf{k}_\perp) &= -\frac{k^1 + ik^2}{xM_N} \varphi_q^{(2)}(x, \mathbf{k}_\perp), \\
 \psi_{+q}^-(x, \mathbf{k}_\perp) &= \frac{k^1 - ik^2}{xM_N} \varphi_q^{(2)}(x, \mathbf{k}_\perp), \\
 \psi_{-q}^-(x, \mathbf{k}_\perp) &= \varphi_q^{(1)}(x, \mathbf{k}_\perp)
 \end{aligned}$$

$$\varphi_q^{(1)}(x, \mathbf{k}_\perp) = \frac{4\pi}{M_N} \sqrt{\frac{q_v(x) + \delta q_v(x)}{2}} \sqrt{D_q^{(1)}(x)} \exp\left[-\frac{\mathbf{k}_\perp^2}{2M_N^2} D_q^{(1)}(x)\right],$$

$$\varphi_q^{(2)}(x, \mathbf{k}_\perp) = \frac{4\pi}{M_N} \sqrt{\frac{q_v(x) - \delta q_v(x)}{2}} D_q^{(2)}(x) \exp\left[-\frac{\mathbf{k}_\perp^2}{2M_N^2} D_q^{(2)}(x)\right].$$

Here M_N is the nucleon mass.

Nucleon as quark-scalar diquark in LFQM

Our functions $\varphi_q^{(1)}$ and $\varphi_q^{(2)}$ are normalized as

$$\begin{aligned}\int \frac{d^2\mathbf{k}_\perp}{16\pi^3} \left[\varphi_q^{(1)}(x, \mathbf{k}_\perp) \right]^2 &= \frac{q_v(x) + \delta q_v(x)}{2}, \\ \int \frac{d^2\mathbf{k}_\perp}{16\pi^3} \frac{\mathbf{k}_\perp^2}{M_N^2} \left[\varphi_q^{(2)}(x, \mathbf{k}_\perp) \right]^2 &= \frac{q_v(x) - \delta q_v(x)}{2}\end{aligned}$$

and

$$\begin{aligned}\int_0^1 dx \int \frac{d^2\mathbf{k}_\perp}{16\pi^3} \left[\varphi_q^{(1)}(x, \mathbf{k}_\perp) \right]^2 &= \frac{n_q + g_A^q}{2}, \\ \int_0^1 dx \int \frac{d^2\mathbf{k}_\perp}{16\pi^3} \frac{\mathbf{k}_\perp^2}{M_N^2} \left[\varphi_q^{(2)}(x, \mathbf{k}_\perp) \right]^2 &= \frac{n_q - g_A^q}{2},\end{aligned}$$

where n_q is the number of u or d valence quarks in the proton and g_A^q is the axial charge of a quark with flavor $q = u$ or d .

Nucleon as quark-scalar diquark in LFQM

LF representation for the Dirac and Pauli quark form factors is

$$\begin{aligned}
 F_1^q(Q^2) &= \int_0^1 dx \int \frac{d^2 \mathbf{k}_\perp}{16\pi^3} \left[\psi_{+q}^{+\ast}(x, \mathbf{k}'_\perp) \psi_{+q}^+(x, \mathbf{k}_\perp) \right. \\
 &\quad \left. + \psi_{-q}^{+\ast}(x, \mathbf{k}'_\perp) \psi_{-q}^+(x, \mathbf{k}_\perp) \right], \\
 F_2^q(Q^2) &= -\frac{2M_N}{q^1 - iq^2} \int_0^1 dx \int \frac{d^2 \mathbf{k}_\perp}{16\pi^3} \\
 &\quad \times \left[\psi_{+q}^{+\ast}(x, \mathbf{k}'_\perp) \psi_{+q}^-(x, \mathbf{k}_\perp) \right. \\
 &\quad \left. + \psi_{-q}^{+\ast}(x, \mathbf{k}'_\perp) \psi_{-q}^-(x, \mathbf{k}_\perp) \right],
 \end{aligned}$$

where $\mathbf{k}'_\perp = \mathbf{k}_\perp + \mathbf{q}_\perp(1-x)$. Here $\psi_{\lambda_q q}^{\lambda_N}(x, \mathbf{k}_\perp)$ are the LFWFs at the initial scale μ_0 with specific helicities for the nucleon $\lambda_N = \pm$ and for the struck quark $\lambda_q = \pm$, where plus and minus correspond to $+\frac{1}{2}$ and $-\frac{1}{2}$, respectively. We work in the frame with $q = (0, 0, \mathbf{q}_\perp)$.

Nucleon as quark-scalar diquark in LFQM

Expressions for the quark helicity-independent NPDs \mathcal{H}^q and \mathcal{E}^q in the nucleon read

$$\begin{aligned}\mathcal{H}^q(x, Q^2) &= \frac{q_v(x) + \delta q_v(x)}{2} e^{-t_q^{(11)}(x, Q^2)} \\ &+ \frac{q_v(x) - \delta q_v(x)}{2} e^{-t_q^{(22)}(x, Q^2)} \\ &\times \left[1 - t_q^{(22)}(x, Q^2) \right], \\ \mathcal{E}^q(x, Q^2) &= \mathcal{E}^q(x) e^{-t_q^{(12)}(x, Q^2)},\end{aligned}$$

where

$$t_q^{(ij)}(x, Q^2) = \frac{Q^2}{4M_N^2} \frac{2D_q^{(i)}(x) D_q^{(j)}(x)}{D_q^{(i)}(x) + D_q^{(j)}(x)} (1-x)^2.$$

The magnetization PDF $\mathcal{E}^q(x)$ reads

$$\mathcal{E}^q(x) = 4\sqrt{q_v^2(x) - \delta q_v^2(x)} \sqrt{D_q^{(1)}(x)} \frac{(1-x)\sigma_q(x)}{\left[1 + \sigma_q(x)\right]^2}, \quad \sigma_q(x) = D_q^{(2)}(x)/D_q^{(1)}(x).$$

Nucleon as quark-scalar diquark in LFQM

$$\begin{aligned} f_1^{qv}(x, \mathbf{k}_\perp) &\equiv h_{1T}^{qv}(x, \mathbf{k}_\perp) \\ &= \frac{1}{16\pi^3} \left[|\psi_{+q}^+(x, \mathbf{k}_\perp)|^2 + |\psi_{-q}^+(x, \mathbf{k}_\perp)|^2 \right] \\ &= \frac{1}{16\pi^3} \left[\left(\varphi_q^{(1)}(x, \mathbf{k}_\perp) \right)^2 + \frac{\mathbf{k}_\perp^2}{M_N^2} \left(\varphi_q^{(2)}(x, \mathbf{k}_\perp) \right)^2 \right], \end{aligned}$$

$$\begin{aligned} g_{1L}^{qv}(x, \mathbf{k}_\perp) &= \frac{1}{16\pi^3} \left[|\psi_{+q}^+(x, \mathbf{k}_\perp)|^2 - |\psi_{-q}^+(x, \mathbf{k}_\perp)|^2 \right] \\ &= \frac{1}{16\pi^3} \left[\left(\varphi_q^{(1)}(x, \mathbf{k}_\perp) \right)^2 - \frac{\mathbf{k}_\perp^2}{M_N^2} \left(\varphi_q^{(2)}(x, \mathbf{k}_\perp) \right)^2 \right], \end{aligned}$$

Nucleon as quark-scalar diquark in LFQM

$$\begin{aligned}
& g_{1T}^{q_v}(x, \mathbf{k}_\perp) \equiv -h_{1L}^{\perp q_v}(x, \mathbf{k}_\perp) \\
= & \frac{1}{16\pi^3} \left[\psi_{+q}^{+*}(x, \mathbf{k}_\perp) \psi_{+q}^{-}(x, \mathbf{k}_\perp) \frac{M_N}{k^1 - ik^2} \right. \\
& + \left. \psi_{+q}^{-*}(x, \mathbf{k}_\perp) \psi_{+q}^{+}(x, \mathbf{k}_\perp) \frac{M_N}{k^1 + ik^2} \right] \\
= & \frac{1}{8\pi^3} \varphi_q^{(1)}(x, \mathbf{k}_\perp) \varphi_q^{(2)}(x, \mathbf{k}_\perp),
\end{aligned}$$

$$\begin{aligned}
h_1^{q_v}(x, \mathbf{k}_\perp) & \equiv h_{1T}^{q_v}(x, \mathbf{k}_\perp) + \frac{\mathbf{k}_\perp^2}{2M_N^2} h_{1T}^{\perp q_v}(x, \mathbf{k}_\perp) \\
= & \frac{1}{2} \left[f_1^{q_v}(x, \mathbf{k}_\perp) + g_{1L}^{q_v}(x, \mathbf{k}_\perp) \right] \\
= & \frac{1}{16\pi^3} |\psi_{+q}^{+}(x, \mathbf{k}_\perp)|^2 = \frac{1}{16\pi^3} \left(\varphi_q^{(1)}(x, \mathbf{k}_\perp) \right)^2,
\end{aligned}$$

Nucleon as quark-scalar diquark in LFQM

$$\begin{aligned} \frac{\mathbf{k}_\perp^2}{2M_N^2} h_{1T}^{\perp q_v}(x, \mathbf{k}_\perp) &= \frac{1}{2} \left[g_{1L}^{q_v}(x, \mathbf{k}_\perp) - f_1^{q_v}(x, \mathbf{k}_\perp) \right] \\ &= g_{1L}^{q_v}(x, \mathbf{k}_\perp) - h_1^{q_v}(x, \mathbf{k}_\perp) \\ &= -\frac{1}{16\pi^3} |\psi_{-q}^+(x, \mathbf{k}_\perp)|^2 \\ &= -\frac{1}{16\pi^3} \frac{\mathbf{k}_\perp^2}{M_N^2} \left(\varphi_q^{(2)}(x, \mathbf{k}_\perp) \right)^2. \end{aligned}$$

Nucleon as quark-scalar diquark in LFQM

Using our expressions for the LFWFs we can express the TMDs through the PDFs

$$\begin{aligned}
f_1^{qv}(x, \mathbf{k}_\perp) &\equiv h_{1T}^{qv}(x, \mathbf{k}_\perp) = \mathcal{F}_1(x, \mathbf{k}_\perp) + \mathcal{F}_2(x, \mathbf{k}_\perp), \\
g_{1L}^{qv}(x, \mathbf{k}_\perp) &= \mathcal{F}_1(x, \mathbf{k}_\perp) - \mathcal{F}_2(x, \mathbf{k}_\perp), \\
g_{1T}^{qv}(x, \mathbf{k}_\perp) &\equiv -h_{1L}^{\perp qv}(x, \mathbf{k}_\perp) = \mathcal{F}_3(x, \mathbf{k}_\perp), \\
h_1^{qv}(x, \mathbf{k}_\perp) &= \mathcal{F}_1(x, \mathbf{k}_\perp), \\
\frac{\mathbf{k}_\perp^2}{2M_N^2} h_{1T}^{\perp qv}(x, \mathbf{k}_\perp) &= -\mathcal{F}_2(x, \mathbf{k}_\perp), \\
\mathcal{F}_1(x, \mathbf{k}_\perp) &= \frac{1}{\pi M_N^2} \frac{q_v(x) + \delta q_v(x)}{2} D_q^{(1)}(x) e^{-\frac{\mathbf{k}_\perp^2}{M_N^2} D_q^{(1)}(x)}, \\
\mathcal{F}_2(x, \mathbf{k}_\perp) &= \frac{1}{\pi M_N^2} \frac{q_v(x) - \delta q_v(x)}{2} \frac{\mathbf{k}_\perp^2}{M_N^2} \left(D_q^{(2)}(x)\right)^2 e^{-\frac{\mathbf{k}_\perp^2}{M_N^2} D_q^{(2)}(x)}, \\
\mathcal{F}_3(x, \mathbf{k}_\perp) &= \sqrt{\frac{4M_N^2}{\mathbf{k}_\perp^2} \mathcal{F}_1(x, \mathbf{k}_\perp) \mathcal{F}_2(x, \mathbf{k}_\perp)} \\
&= \frac{1}{\pi M_N^2} \sqrt{q_v^2(x) - \delta q_v^2(x)} \sqrt{D_q^{(1)}(x)} D_q^{(2)}(x) e^{-\frac{\mathbf{k}_\perp^2}{2M_N^2} \left(D_q^{(1)}(x) + D_q^{(2)}(x)\right)}.
\end{aligned}$$

Nucleon as quark-scalar diquark in LFQM

Wigner distributions

$$\rho^{q[\Gamma]}(x, \mathbf{b}_\perp, \mathbf{k}_\perp; S) = \int \frac{d^2 \Delta_\perp}{4\pi^2} e^{-i \Delta_\perp \mathbf{b}_\perp} W^{q[\Gamma]}(x, \Delta_\perp, \mathbf{k}_\perp; S),$$

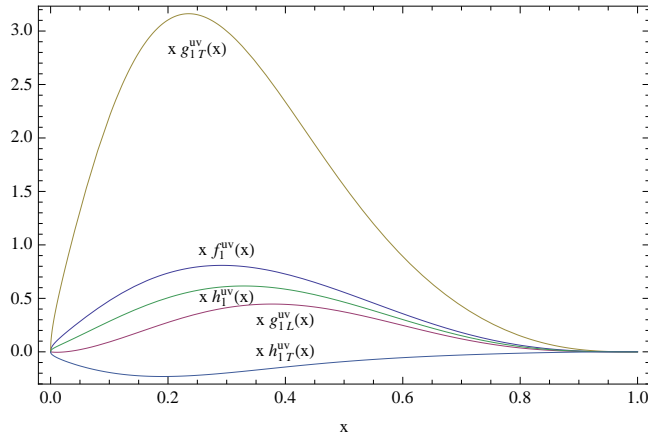
where $W^{q[\Gamma]}(x, \Delta_\perp, \mathbf{k}_\perp; S)$ is the matrix element of the Wigner operator for $\Delta^+ = 0$ and $z^+ = 0$. The light-front decomposition of the Wigner matrix elements $W^{q[\Gamma]}(x, \Delta_\perp, \mathbf{k}_\perp; S)$ is given by

$$W^{q[\gamma^+]}(x, \Delta_\perp, \mathbf{k}_\perp; \pm e_z) = \frac{1}{16\pi^3} \left[\psi_{q+}^{\pm\dagger}(x, \mathbf{k}_\perp^+) \psi_{q+}^\pm(x, \mathbf{k}_\perp^-) + \psi_{q-}^{\pm\dagger}(x, \mathbf{k}_\perp^+) \psi_{q-}^\pm(x, \mathbf{k}_\perp^-) \right],$$

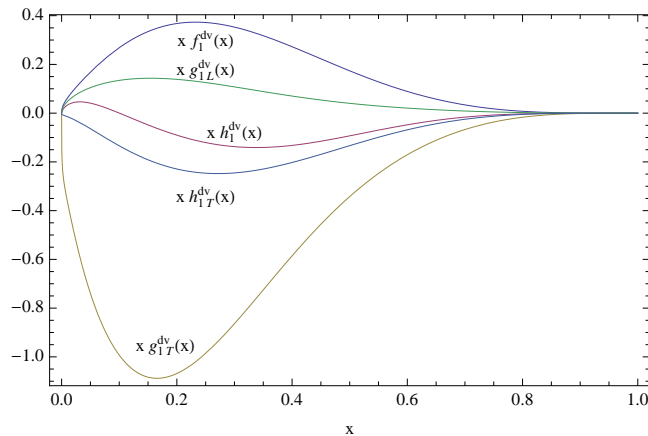
$$W^{q[\gamma^+ \gamma^5]}(x, \Delta_\perp, \mathbf{k}_\perp; \pm e_z) = \frac{1}{16\pi^3} \left[\psi_{+q}^{\pm\dagger}(x, \mathbf{k}_\perp^+) \psi_{+q}^\pm(x, \mathbf{k}_\perp^-) - \psi_{-q}^{\pm\dagger}(x, \mathbf{k}_\perp^+) \psi_{-q}^\pm(x, \mathbf{k}_\perp^-) \right],$$

where $\mathbf{k}_\perp^\pm = \mathbf{k}_\perp \pm (1-x)\Delta_\perp/2$

Nucleon as quark-scalar diquark in LFQM

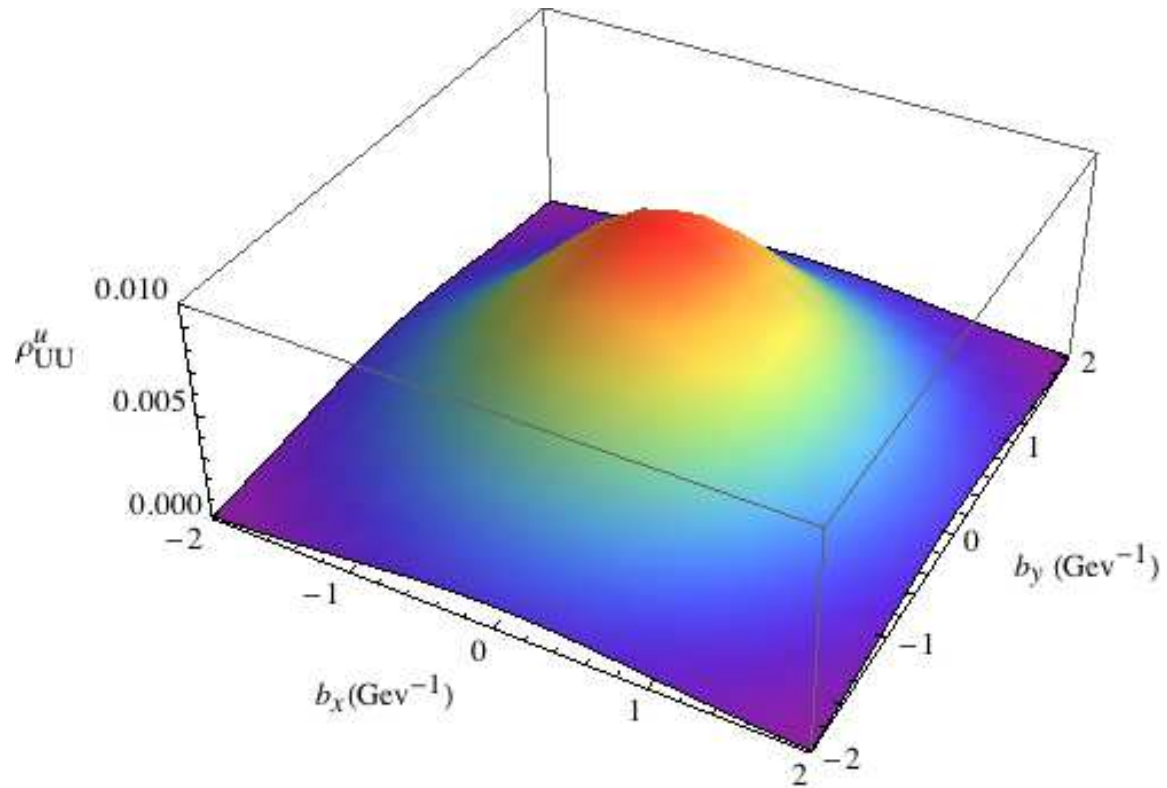


u quark TMDs multiplied with x .



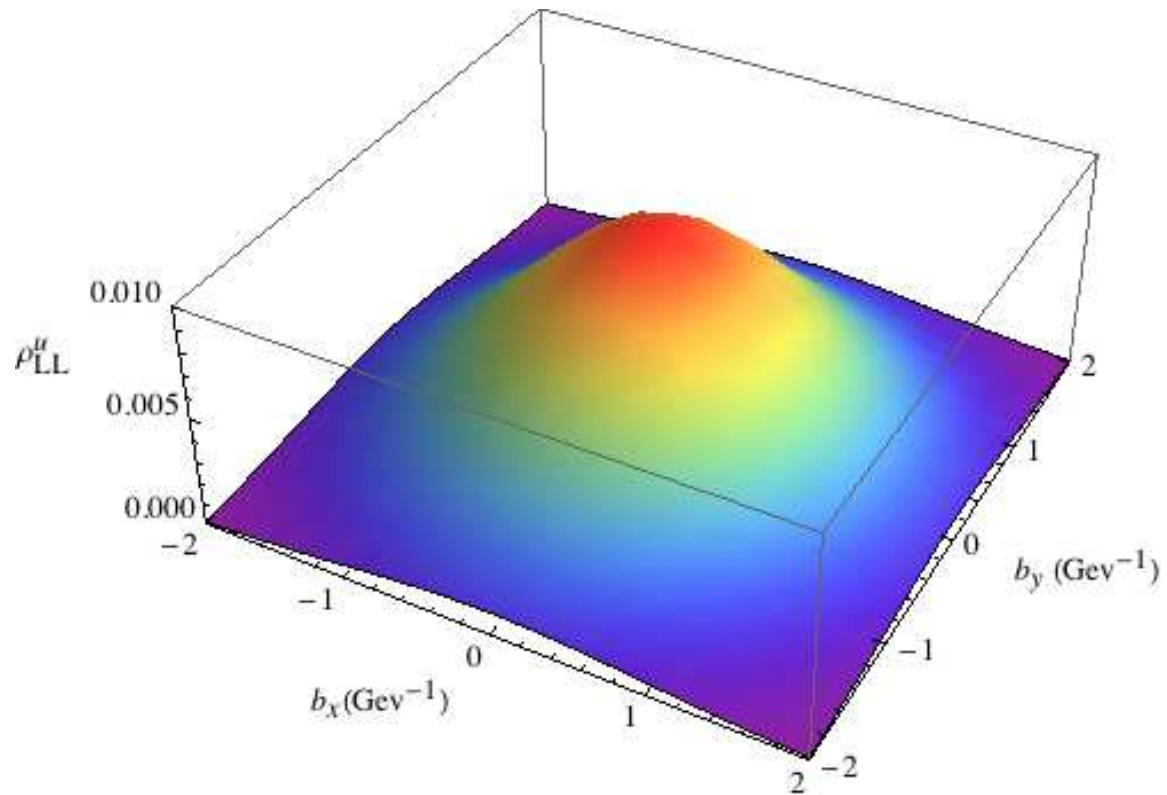
d quark TMDs multiplied with x .

Nucleon as quark-scalar diquark in LFQM



Wigner distribution $\rho_{UU}^u(x, \mathbf{b}_\perp, \mathbf{k}_\perp)$ at $x = 0.5$, $k_x = k_y = 0.5$ GeV.

Nucleon as quark-scalar diquark in LFQM



Wigner distribution $\rho_{LL}^u(x, \mathbf{b}_\perp, \mathbf{k}_\perp)$ at $x = 0.5$, $k_x = k_y = 0.5$ GeV.

Summary

- Lattice certainly complements/helps to experiment and EFTs:
 - quark interpolating currents
 - running quark mass
- EFTs develop own novel ideas